

# Investigation of the correlation between structural relaxation time and configurational entropy under high pressure in a chlorinated biphenyl

R. Casalini<sup>a)</sup>

Naval Research Laboratory, Chemistry Division, Code 6120, Washington, D.C. 20375-5342  
and George Mason University, Chemistry Department, Fairfax, Virginia

M. Paluch

Naval Research Laboratory, Chemistry Division, Code 6120, Washington, D.C. 20375-5342  
and Institute of Physics, Silesian University, Uniwersytecka 4, 40-007 Katowice, Poland

J. J. Fontanella

Physics Department, U.S. Naval Academy, Annapolis, Maryland 21402-5026

C. M. Roland<sup>b)</sup>

Naval Research Laboratory, Chemistry Division, Code 6120, Washington, D.C. 20375-5342

(Received 12 March 2002; accepted 17 June 2002)

Dielectric relaxation measurements on a chlorinated biphenyl (PCB62) were carried out over a broad frequency range, with variation of both temperature and pressure. In combination with calorimetric determinations of the configurational entropy, these data could be described using the Adam–Gibbs model. Specifically, the experimental results were interpreted using a recently introduced equation for both the temperature and pressure dependencies of the structural relaxation time. The  $\tau(T,P)$  data for PCB62 yielded values of the fitting parameters consistent with known physical properties of the material. A change of the dynamics was evident in isobaric measurements at atmospheric pressure, corresponding to a value of the relaxation time  $\tau_B \sim 5 \times 10^{-5}$  s. A related change of dynamics was observed in isothermal experiments at varying pressures. It is noteworthy that the latter transpired at a very similar  $\tau \sim \tau_B$ . Moreover, the shape of the relaxation function depended only on the value of  $\tau$ . We believe this is the first reported evidence of such a change of dynamics in experiments using pressure as a variable. These results suggest that this change is governed by the time scale of the relaxation, independently of any particular combination of  $T$  and  $P$ . © 2002 American Institute of Physics. [DOI: 10.1063/1.1499484]

## INTRODUCTION

The making of glass was practiced in Mesopotamia from about 3000 BC, and glasses have been widely utilized ever since. In particular, with syntheses of numerous new materials in the last century, glasses have become ubiquitous in everyday life. Nevertheless, the nature of the transition from a liquid to the glassy state is not yet fully understood.

While the thermodynamics of a liquid's transformation into a crystalline or gaseous state can be successfully explained, the role of thermodynamics in the glass transition is controversial. The best known interpretation of the glass transition in terms of thermodynamic variables is the Adam–Gibbs (AG) theory,<sup>1</sup> based on the concept of “cooperatively rearranging regions” (CRR) of molecules or polymer segments. According to the AG model, molecules are “forced” to act cooperatively, whereby the characteristic time of the ensemble is related to the characteristic time for molecules to rearrange within a CRR. The latter quantity depends on the number of configurations available, and therefore to the configurational entropy,  $S_c$ . In the AG theory, the progressive slowing down of molecular motions which precipitates the

glass transition is attributed to a decrease of  $S_c$ . This, in turn, is related to the number of configurations,  $\Omega$ , according to  $S_c = k_B \ln \Omega$ , where  $k_B$  is the Boltzmann constant.

Of course, the role of configurational entropy in the glass transition is not limited to the AG model, but underlies the interpretation of this phenomenon by various theories. An example is the energy landscape description,<sup>2,3</sup> according to which approach towards the glass transition causes the system to be progressively trapped within deeper energy minima. The dynamics is governed by the number of such minima and their energy spread. In principle, knowledge of this potential energy hypersurface allows determination of  $S_c$ .<sup>4,5</sup> Simulations using this formalism suggest some validity for a relationship between dynamics and  $S_c$  [Eq. (1)], consistent with the AG model, but without invoking cooperativity.<sup>4</sup> On the other hand, experimental results for polymers<sup>6–10</sup> are at odds with the energy landscape approach per se.

An experimental procedure to determine  $S_c$  is to consider the configurational entropy as equal to the excess entropy of the melt with respect to the crystal,  $S_{ex}$ . As pointed out by Goldstein,<sup>11</sup> this  $S_{ex}$  may include contributions from vibrational and anharmonic forces, thus potentially overestimating  $S_c$  by as much as 40%. Nevertheless, tests of the AG theory using  $S_{ex}$  have been successful for temperatures not

<sup>a)</sup>Electronic mail: [casalini@ccs.nrl.navy.mil](mailto:casalini@ccs.nrl.navy.mil)

<sup>b)</sup>Electronic mail: [roland@nrl.navy.mil](mailto:roland@nrl.navy.mil)

too far for  $T_g$ ,<sup>12–15</sup> presumably due to a proportionality between  $S_c$  and  $S_{ex}$ ,<sup>16</sup> as supported by computer simulation.<sup>17,18</sup>

From an experimental point of view, it is useful to verify whether the change of entropy, as predicted in the AG model, can be related to the structural dynamics, when temperature, and even pressure, are varied. Recently an equation describing the temperature and pressure behavior of the structural relaxation time,  $\tau(T,P)$ , was derived<sup>19</sup> from the AG equation,<sup>1</sup>

$$\tau = \tau_0 \exp(C/TS_c), \quad (1)$$

where  $C$  is a constant proportional to the free energy barrier (per molecule in the cooperative rearranging region),  $\tau_0$  is a constant having the dimensions of time and  $S_c$  is defined as the excess entropy. The derivation considers both temperature and pressure dependences of the configurational entropy,

$$S_c(T,P) = \Delta S_{fus} + \int_{T_K}^T \frac{\Delta C_p(T')}{T'} dT' - \int_0^P \Delta \left( \frac{\partial V}{\partial T} \right)_{P'} dP', \quad (2)$$

where  $\Delta S_{fus}$  is the entropy of fusion, the first integral is related to the excess molar heat capacity,  $\Delta C_p = C_p^{melt} - C_p^{crystal}$ , of the melt relative to the crystal, and the second integral can be expressed in terms of the excess molar thermal expansion,

$$\Delta \left( \frac{\partial V}{\partial T} \right)_{P'} = \left( \frac{\partial \Delta V}{\partial T} \right)_{P'} = \left( \frac{\partial (V^{melt} - V^{crystal})}{\partial T} \right)_{P'}.$$

At atmospheric pressure ( $P \sim 0$ ), the second integral is zero, and since the temperature dependence of the excess heat capacity can be described over a limited range above  $T_g$  by  $\Delta C_p(T) = k/T$ , then  $S_c(T) = S_\infty - k/T$ , where  $k$  is a constant and  $S_\infty$  is the limit of  $S_c$  at very high temperatures.<sup>15</sup> By substituting this equation into Eq. (1), a Vogel–Fulcher (VF)<sup>20,21</sup> expression for the temperature dependence of the relaxation time is obtained  $\tau(T) = \tau_0 \exp(DT_0/(T-T_0))$ ,

where  $T_0$  is the Vogel temperature ( $T_0 = k/S_\infty$ ) and  $D$  ( $D = C/k$ ) is the fragility parameter. It is well known that such an equation describes  $\tau(T)$  for a wide range of materials.

At pressures above atmospheric, the second integral of Eq. (2), describing the isothermal reduction of  $S_c$ , is non-negligible. By substituting Eq. (2) into Eq. (1), a VF-type equation for  $\tau(T,P)$  is obtained again, with the Vogel temperature now defined as

$$T_0^*(T,P) = \frac{T_0}{1 - \frac{1}{S_\infty} \int_0^P \Delta \left( \frac{\partial V}{\partial T} \right)_{P'} dP'}. \quad (3)$$

According to this approach, the fragility parameter  $D$  is independent of pressure (assuming the free energy barrier to rearrangements remains constant). As a consequence, if the temperature dependence of the excess expansivity integral is negligible,  $T_0^*$  depends only on pressure, and  $\tau(T,P)$  data at a fixed pressure should be described by a VF equation having the same fragility parameter  $D$ .

A common parameter used to describe the fragility of a glassformer is the steepness index  $m = (d \log(\tau)/d(T_g/T))_{T=T_g}$ . If the VF equation applies, it follows<sup>22</sup> that if  $D$  and  $\tau_0$  are constant, then the  $m$  is constant. Consequently, in the proposed “extension” of the AG model, if the temperature dependence of the function  $T_0^*$  is negligible, then the fragility must be independent of pressure.

To arrive at a more accessible form for  $T_0^*$ , the integral in Eq. (3) was calculated using the Tait equation<sup>23–25</sup> to describe the temperature and pressure dependence of the volume,  $V(T,P) = V(T,0)[1 - C \ln(1 + P/B(T))]$ , where  $C$  is a constant (average value  $C = 8.92 \times 10^{-2}$ ) and  $B(T)$  has the dimensions of pressure.<sup>25,26</sup> The temperature dependence of  $B(T)$  is well described by  $B(T) = b_1 \exp(-b_2 T)$ , with average values  $b_1 = 300$  MPa and  $b_2 = 4 \times 10^{-3} \text{ K}^{-1}$ .<sup>25,26</sup>

This leads to the following expression for  $T_0^*(T,P)$ :<sup>19</sup>

$$T_0^*(T,P) = \frac{T_0}{1 + \left( \frac{\delta}{S_\infty} \right) \left\{ -(\beta + \gamma - 1)P + [(\gamma - 1)B(T) + \gamma P] \ln \left( 1 + \frac{P}{B(T)} \right) \right\}}, \quad (4)$$

where  $\delta = CV^{melt}(T,0)b_2$ ,  $\beta = \delta^{-1} \Delta(\partial V/\partial T)_{P=0}$ , and  $\gamma = \alpha/b_2$ , with  $\alpha$  being the thermal expansion coefficient of the melt.

## EXPERIMENT

A polychlorinated biphenyl having 62% by weight chlorine (obtained from J. Schrag and manufactured by Monsanto) is referred herein as PCB62. PCB's are a mixture of biphenyls, containing from one to nine chlorines per molecule. The presence of the various homologs suppresses crystallization. The primary species in PCB62 is heptachlorobiphenyl.

Dielectric measurements were carried out over 13 decades of frequency ( $10^{-4}$ – $10^9$  Hz), using an IMASS time domain dielectric analyzer ( $10^{-4}$ – $10^4$  Hz), a HP4284A LCR meter ( $2 \times 10^1$ – $10^6$  Hz) and an HP491A impedance analyzer ( $10^6$ – $10^9$  Hz). Measurements at elevated pressure were limited to a narrower frequency range ( $10^{-4}$ – $10^6$  Hz).

The sample cell for frequencies below  $10^6$  Hz was a parallel plate capacitor, placed in an oven (nitrogen atmosphere) in which the temperature was controlled within  $\pm 0.1$  K. For the high pressure measurements, the capacitor (geometric capacitance  $\sim 35$  pF) was isolated from the pressurizing fluid by means of a Teflon ring. Pressure was applied

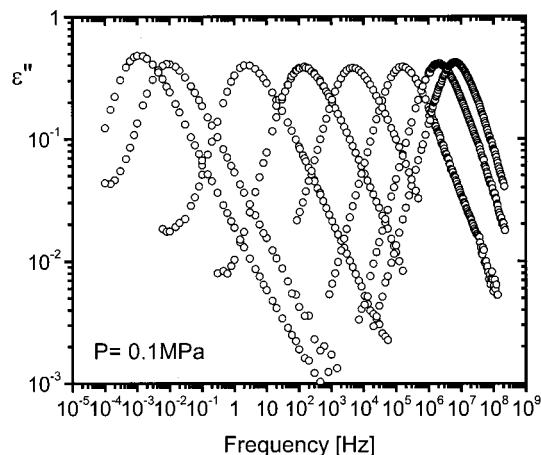


FIG. 1. Dielectric loss spectra of PCB62 measured at various temperatures and atmospheric pressure. The temperatures are (from left to right): 267, 272.1, 284.1, 294.1, 304.1, 316.5, 329.1, and 336.6 K.

using a hydraulic pump, and measured with a Sensotec tensometric transducer (resolution = 150 kPa). Measurements above  $10^6$  Hz were carried out using an HP16453A test fixture.

Differential scanning calorimetry employed a Perkin Elmer DSC7.

## RESULTS AND DISCUSSION

The dielectric loss ( $\epsilon''$ ) spectra of PCB62 at atmospheric pressure (Fig. 1), show the presence of the structural (or  $\alpha$ ) relaxation, which progressively slows down and becomes broader with decreasing temperature. While a well-resolved secondary peak is never observed, at temperatures close to and below the glass transition temperature ( $T_g$ ), an extra contribution can be seen on the high frequency side of the  $\alpha$  relaxation. A detailed analysis of this excess intensity has been reported elsewhere.<sup>27</sup> In the present paper, we restrict our attention to the temperature and pressure dependencies of the structural dynamics. Given the broad range of accessible frequencies, it is possible to follow the dynamics over an interval of about  $116^\circ$ , which corresponds to a change in the structural relaxation time of more than 12 decades. Dielectric loss spectra measured as a function of pressure at constant temperature (Fig. 2) reveal the high sensitivity of the structural relaxation dynamics of PCB62 to pressure. Moreover, similar to isobaric data obtained by varying temperature, the spectra become broader with increasing magnitude of the relaxation time.

By comparing spectra measured for different conditions of temperature and pressure, but having the same relaxation time, it can be seen that the shape of the  $\alpha$  relaxation spectrum is a unique function of  $\tau$ . We illustrate this in Fig. 3, showing three pairs of spectra having the same  $\tau$ , measured, respectively, at atmospheric pressure for  $T = 284.1$ , 301.6, and 316.5 K, and at  $T = 334.5$  K for  $P = 161.6$ , 92.6, and 46 MPa. Although such superposition of isobaric and isothermal data has been observed previously for other glassformers,<sup>28–30</sup> it is particularly striking herein, given the strong dependence of the peak breadth on  $\tau$ .

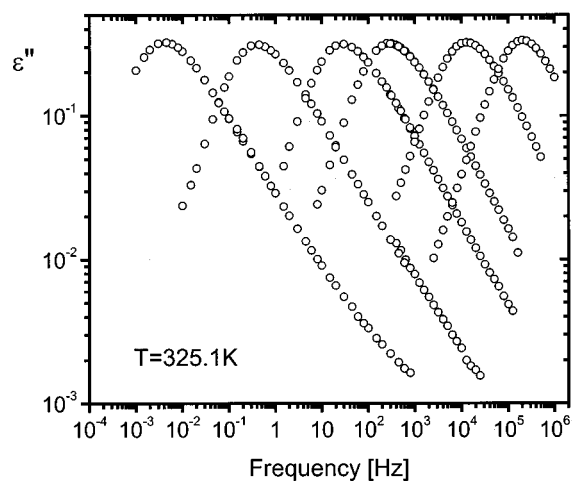


FIG. 2. Dielectric loss spectra of PCB62 measured at various pressures at  $T = 325.1$  K. The pressures are (from right to left): 20.9, 50.3, 86.8, 149.0, and 192.0 MPa.

This progressive broadening of the  $\alpha$  relaxation is shown in the inset to Fig. 3, in which the full width at half maximum (FWHM) of the loss peak is plotted as a function of the relaxation time  $\tau$  ( $= 1/2\pi f$ ), for both isobaric and isothermal experiments. It is evident that the spectra measured for different conditions of temperature and pressure exhibit the same behavior. This peak breadth (at fixed  $\tau$ ) is well-known to correlate with  $m$ ,<sup>31–36</sup> although there are exceptions.<sup>30,37–41</sup> If the correlation obtains herein, then the fragility should not change over the investigated range of pressures, as has been seen for several glassformers.<sup>22,29,41–43</sup> On

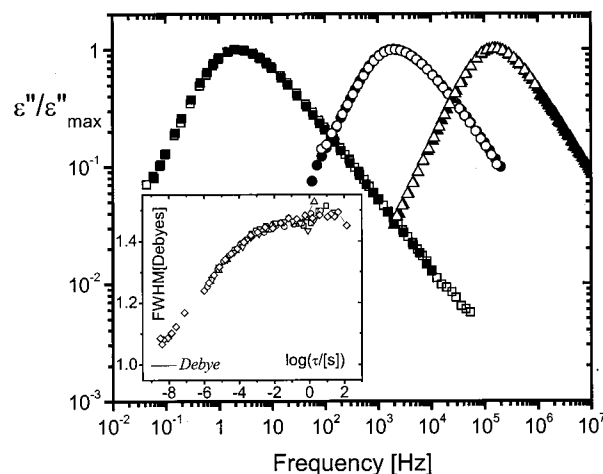


FIG. 3. Comparison of dielectric loss of PCB62 measured for different combinations of temperature and pressure having the same relaxation time. The spectra were normalized by the maximum in their respective  $\epsilon''$ . Three spectra were measured at atmospheric pressure (solid symbols) and (from left to right)  $T = 284.1$  K,  $T = 301.6$  K, and  $T = 316.5$  K, respectively, while the other three were measured at  $T = 334.5$  K (open symbols) and (from left to right)  $P = 161.6$  MPa,  $P = 92.6$  MPa, and  $P = 46$  MPa, respectively. In the inset are the full widths at half maximum (relative to Debye relaxation) plotted vs the relaxation time. These data refer to the FWHM of spectra measured at various temperatures at atmospheric pressure (0.1 MPa) ( $\diamond$ ), and spectra measured at various pressures at  $T = 296.1$  K ( $\square$ ),  $T = 325.1$  K ( $\circ$ ),  $T = 334.5$  K ( $\triangle$ ), and  $T = 344$  K ( $\nabla$ ), respectively.

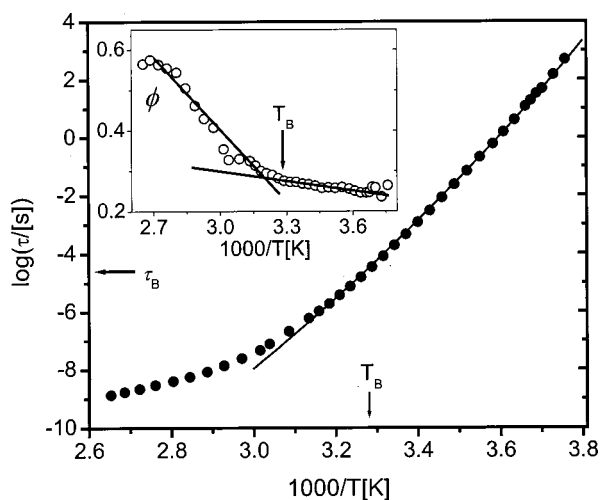


FIG. 4. Structural relaxation time of PCB62 measured at atmospheric pressure. The solid line is the best fit obtained by fitting the data to the VF equation with  $T_0$  substituted by the function  $T_0^*(T,P)$  [Eq. (4)]. The inset shows the Stickel function  $\phi = (d \log(\tau)/d(1000/T))^{-1/2}$ . The solid lines serve to emphasize the change of dynamics at  $T_B$  from the VF behavior observed for  $T_g < T < T_B$ .

the other hand, for glycerol, it was recently shown that an increase of pressure gives rise to both an increase in fragility and broadening of the  $\alpha$  relaxation.<sup>44</sup>

The temperature dependence of the structural relaxation time measured at atmospheric pressure is shown in Fig. 4. A common method for analyzing such data is to use the Stickel function  $\phi = (d \log(\tau)/d(1000/T))^{-1/2}$ .<sup>45</sup>  $\phi$  transforms a VF behavior into a straight line, and an Arrhenius behavior into a constant. More importantly,  $\phi$  facilitates determination of any deviations from a single VF relation. In the inset to Fig. 4,  $\phi$  for the PCB62 data is displayed, making evident a deviation from the low temperature VF behavior at a temperature  $T_B \sim 315$  K ( $T_B/T_g \sim 1.14$ ); this corresponds to a value of  $\tau (\equiv \tau_B) \sim 5 \times 10^{-5}$  s.

Figure 5 shows the isothermal pressure dependence of the structural relaxation time for seven temperatures ( $T = 296.1, 303.4, 311.7, 317.4, 325.1, 334.5$ , and  $344$  K). A strong sensitivity of  $\tau$  to pressure is apparent. In fact, at the lowest temperature,  $\tau$  changes by more than four orders of magnitude for a pressure change of only 80 MPa. These results demonstrate that a sensitivity of the structural relaxation time to pressure is not necessarily associated with large fragility. For example, the fragility of glycerol [ $m = 53$  (Ref. 32)] is not far from that of PCB62 ( $m = 63$ ); however, the structural relaxation of the former is much more insensitive to pressure.<sup>44</sup>

An analysis of the pressure and temperature dependences of  $\tau(T,P)$  was carried out by substituting  $T_0$  with the function  $T_0^*(T,P)$  [Eq. (4)] in the VF equation and simultaneously fitting the data in Figs. 4 and 5. We restricted the fit to  $\tau$  longer than the relaxation time  $\tau_B$ , ( $\sim 5 \times 10^{-5}$  s). The parameters  $\delta = 8.55 \times 10^{-2} \text{ MPa}^{-1}$  and  $\gamma = 0.16$  in Eq. (4) were calculated from the known physical properties of PCB62: density =  $1.577 \text{ g cm}^{-3}$ , molecular weight =  $376.6 \text{ g mol}^{-1}$ , and  $\alpha = 6.4 \times 10^{-4} \text{ K}^{-1}$ . We used average liquid

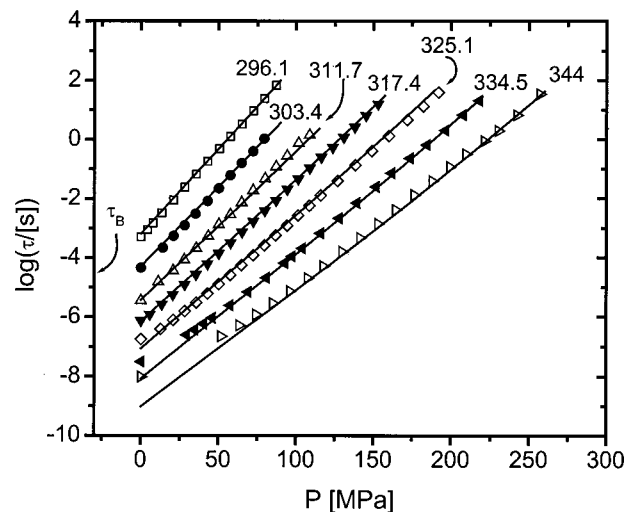


FIG. 5. Structural relaxation time of PCB62 vs pressure for seven temperatures (indicated in K in the figure). The solid line is the best fit of the data to a VF equation with  $T_0$  substituted by the function  $T_0^*(T,P)$  [Eq. (4)]. Note that the fit was carried out only for  $\tau > \tau_B$ , although we show the calculated curve for shorter  $\tau$  to emphasize the deviation at lower pressure for the higher temperatures.

values for  $b_2 = 4 \times 10^{-3} \text{ K}^{-1}$  and  $C = 8.94 \times 10^{-2}$ . Any temperature dependence of the parameter  $B$  was neglected, with its value taken to be 260 MPa. (Note that over this range of pressures, the particular value of  $B$  has minimal influence on the calculation.<sup>46</sup>)

In Figs. 4 and 5, the best fit of the AG model is displayed as solid lines. The obtained parameters were  $\log(\tau_0/[s]) = -23.8 \pm 1.3$ ,  $D = 40 \pm 7$ ,  $T_0 = 160 \pm 7$  K,  $\beta = 1.3 \pm 0.2$ , and  $S_\infty = 95 \pm 5 \text{ J mol}^{-1} \text{ K}^{-1}$ . This value of  $S_\infty$  is the same order of magnitude as values obtained for other glassformers,<sup>15</sup> while the value of  $\beta$  is consistent with its known physical properties; to wit,  $\beta < \delta^{-1} V^{\text{melt}}(T,0) \alpha = \alpha / C b_2 = 1.79$ . The obtained value for  $\tau_0$  is clearly smaller than the time scale of any molecular motion. However, the quantity  $C$  in Eq. (1) is proportional to an effective energy barrier represented by the Gibbs free energy, such that the actual noncooperative relaxation time at high temperature is longer than  $\tau_0$ . Indeed, from Fig. 5 it is evident that for the isotherms at higher temperature, an extrapolation of the fit for  $\tau < \tau_B$  deviates from the experimental results. This is similar to the manner in which the VF fails to describe the atmospheric pressure data over the entire temperature range (Fig. 4). Thus, the change of dynamics observed at  $T_B$  in a Stickel plot is also manifested upon application of pressure. The deviation occurs in both cases at a characteristic value of the relaxation time,  $\tau \sim \tau_B \sim 5 \times 10^{-5}$  s.

From the extension of the AG model, it is possible to predict the pressure dependence of  $T_g$ . In fact, if the temperature dependence of  $T_0^*(T,P)$  can be neglected (over the investigated range of pressure and temperature), we can obtain a relation for  $T_g$  [defined for our purposes as the temperature at which  $\log(\tau)$  is an arbitrary constant,  $a$ ]. Combining the VF expression and Eq. (4), it follows that

$$T_g(P) = T_0^*(P)(1 + a^*)/a^*, \quad (5)$$

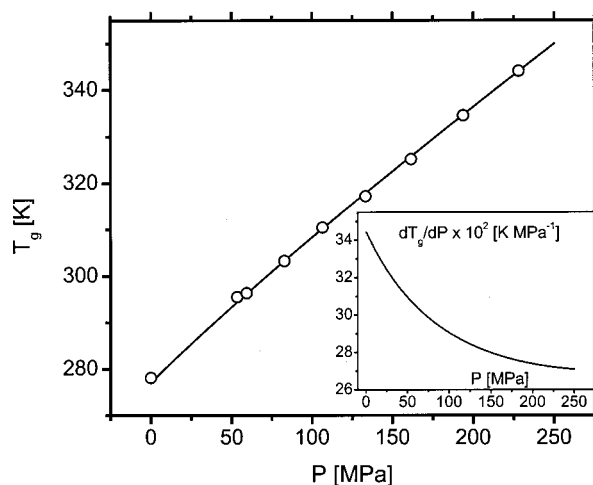


FIG. 6. Pressure dependence of the glass transition temperature  $T_g(P)$ , taken here as the temperature for which  $f_{\max} = 10^{-1}$  Hz (so that no extrapolation was necessary). The points are from the measured relaxation times, while the solid line is calculated from the AG model [Eq. (4)], using parameters estimated from the fit of the  $\tau(T, P)$  data. The inset shows the derivative of the latter.

where  $a^* = (a - \log(\tau_0)) / (D \log(e))$ . Thus, the pressure dependence of  $T_0^*$  yields an expression for the pressure dependence of  $T_g$ .

In Fig. 6 we show  $T_g(P)$  [taking  $a = -\log(2\pi \cdot 10^{-1})$ ] obtained directly from the experimental data, along with the  $T_0^*$  [Eq. (4)], calculated from the parameters obtained by fitting the AG model to the  $\tau(T, P)$  data. The nonlinearity of the pressure dependence of  $T_g$  is noted in the inset to Fig. 6, which shows the derivative of  $T_g(P)$  calculated from the AG model.

In Fig. 7 is displayed the molar heat capacity of PCB62 measured at atmospheric pressure during cooling at  $10 \text{ K min}^{-1}$ . To calculate  $S_c$  at atmospheric pressure from Eq. (2) [ $P \sim 0$ , second integral in Eq. (2) negligible], it would be necessary to measure the thermal heat capacity of the crystal,

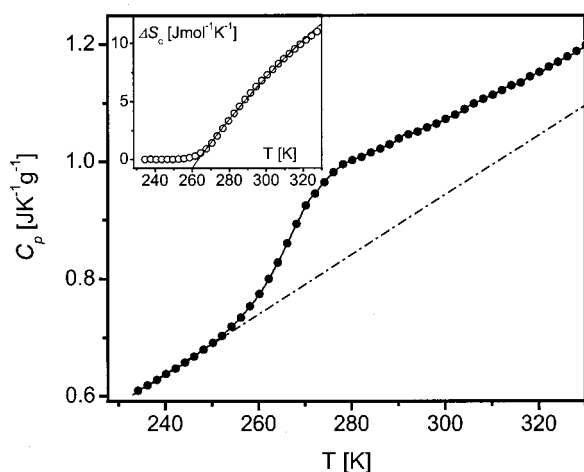


FIG. 7. Heat capacity for PCB62 measured during cooling at  $10 \text{ K min}^{-1}$ . The dashed line indicates a linear extrapolation of  $C_p^{\text{glass}}$  for  $T > T_g$ . The inset shows the entropy of the melt over that of the glass,  $\Delta S_c$  ( $\circ$ ), calculated as discussed in the text. The solid line is the fit for  $T > T_g$  of the function  $\Delta S_c = S_1 - k_1/T$ .

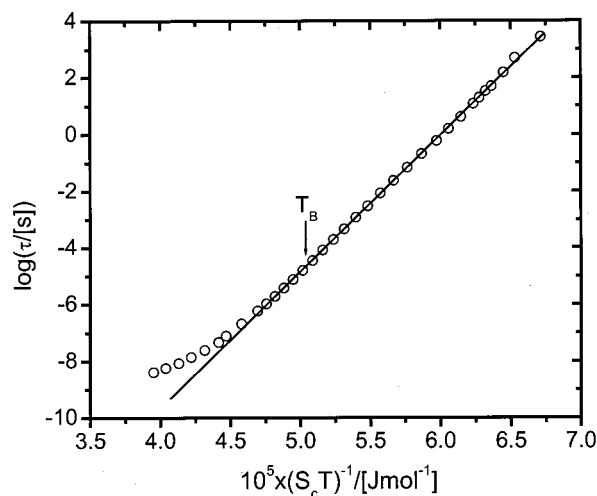


FIG. 8. Structural relaxation times measured at atmospheric pressure. The solid line illustrates the agreement with the AG model [Eq. (2)] observed for lower temperatures ( $T < T_B$ ).

which is not possible for amorphous PCB62. Therefore, we calculated the excess heat capacity of the melt with respect to the glass,  $\Delta C_p^{\text{glass}} = C_p^{\text{melt}} - C_p^{\text{glass}}$ , assuming linear behavior for  $C_p^{\text{glass}}$  at temperatures above  $T_g$ . By integrating  $\Delta C_p^{\text{glass}}/T$ , we obtain the excess entropy of the melt with respect to the crystal,  $\Delta S_c$ . The latter quantity is expected to exhibit temperature behavior very close to that of  $S_c$  for  $T > T_g$ , as shown experimentally.<sup>47</sup> Simulations likewise indicated that  $\Delta S_c$  is a good approximation to  $S_c$ .<sup>5,18</sup> Thus, we take  $\Delta S_c = S_1 - k_1/T$ , with  $k_1 \sim k$  and  $S_1 < S_\infty$ .

The inset of Fig. 7 shows  $\Delta S_c$ , along with the best fit to the previous equation obtained for  $S_1 = 58 \pm 0.1 \text{ J mol}^{-1} \text{ K}^{-1}$  and  $k_1 = 15270 \pm 30 \text{ J mol}^{-1}$ . Using the value of  $k_1$  estimated from  $\Delta S_c$  and the  $T_0$  deduced from the  $\tau(T, P)$  data, we calculate  $S_\infty = k_1/T_0 = 115 \pm 3 \text{ J mol}^{-1} \text{ K}^{-1}$ . This is in agreement with the value,  $S_\infty = 110 \pm 15 \text{ J mol}^{-1} \text{ K}^{-1}$ , determined from our fit of the  $\tau(T, P)$  data to the AG model.

This analysis also demonstrates that by calculating  $S_\infty$  from calorimetry measurements, the number of adjustable parameters in fitting the  $\tau(T, P)$  data can be reduced from five to four.<sup>48</sup> Note also that the  $S_c$  so determined is independent of the actual value of  $S_{\text{ex}}$ , thus avoiding problems related to the determination of anharmonic contributions, as well as the unavailability of values for  $C_p^{\text{crystal}}$ .

By adding  $S_\infty - S_1$  to the calculated  $\Delta S_c$ , we can estimate  $S_c(T, 0)$ ; the results are shown in Fig. 8. It is evident that for longer  $\tau$ , the linear behavior predicted by the AG model [Eq. (1)] is observed; however, there is a deviation at shorter times. Nonlinearity arises at values of  $\tau$  about equal to  $\tau_B$ , associated with the change of dynamics seen in Fig. 3. Thus, time scale is again seen to be the parameter governing the crossover in dynamics.

## CONCLUSIONS

Isothermal and isobaric dielectric relaxation measurements on a chlorinated biphenyl (PCB62) were carried out over a broad range of frequency. Using calorimetric determi-

nations of the configurational entropy, these data could be described using the AG model [Eq. (1)]. Specifically, the experimental results were interpreted using a recently introduced equation<sup>19</sup> which describes both temperature and pressure dependencies of the structural relaxation time. The  $\tau(T,P)$  data for PCB62 yielded values of the fitting parameters consistent with the known physical properties of the material. Moreover, the  $S_\infty$  obtained from calorimetric measurements is in good agreement with the value of the configurational entropy deduced from the  $\tau(T,P)$  data.

The customary change of dynamics was seen in the measurements at atmospheric pressure, at a value of the relaxation time  $\tau_B \sim 5 \times 10^{-5}$  s. The same change of dynamics was likewise observed in measurements at elevated pressures. It is noteworthy that the latter transpired at a similar value of  $\tau \sim \tau_B$ . This suggests that the variable controlling the onset of this crossover in behavior is neither temperature nor pressure, but rather the time scale of the molecular motion.

## ACKNOWLEDGMENT

The work at the NRL and (in part) at USNA is supported by the Office of Naval Research.

- <sup>1</sup>G. Adam and J. H. Gibbs, *J. Chem. Phys.* **43**, 139 (1965).
- <sup>2</sup>M. Goldstein, *J. Chem. Phys.* **51**, 3728 (1969).
- <sup>3</sup>C. A. Angell, *Science* **267**, 1924 (1995).
- <sup>4</sup>S. Sastry, *Nature (London)* **409**, 164 (2001).
- <sup>5</sup>F. Sciortino, W. Kob, and P. Tartaglia, *Phys. Rev. Lett.* **83**, 3214 (1999).
- <sup>6</sup>C. M. Roland, P. G. Santangelo, and K. L. Ngai, *J. Chem. Phys.* **111**, 5593 (1999).
- <sup>7</sup>P. G. Santangelo and C. M. Roland, *Macromolecules* **31**, 4581 (1998).
- <sup>8</sup>P. G. Santangelo and C. M. Roland, *Phys. Rev. B* **58**, 14121 (1998).
- <sup>9</sup>C. M. Roland, P. G. Santangelo, M. Antonietti, and M. Neese, *Macromolecules* **32**, 2283 (1999).
- <sup>10</sup>M. J. Schroeder, C. M. Roland, and T. K. Kwei, *Macromolecules* **32**, 6249 (1999).
- <sup>11</sup>M. Goldstein, *J. Chem. Phys.* **64**, 4767 (1975).
- <sup>12</sup>J. H. Magill, *J. Chem. Phys.* **47**, 4802 (1967).
- <sup>13</sup>S. Takahara, O. Yamamuro, and H. Suga, *J. Non-Cryst. Solids* **171**, 259 (1994).
- <sup>14</sup>S. Takahara, O. Yamamuro, and T. Matsuo, *J. Phys. Chem.* **99**, 9580 (1995).
- <sup>15</sup>R. Richert and C. A. Angell, *J. Chem. Phys.* **108**, 9016 (1998).
- <sup>16</sup>L. M. Martinez and C. A. Angell, *Nature (London)* **410**, 663 (2000).
- <sup>17</sup>F. W. Starr, S. Sastry, E. La Nave, A. Scala, H. E. Stanley, and F. Sciortino, *Phys. Rev. E* **63**, 041201 (2001).
- <sup>18</sup>S. Kamath, R. H. Colby, S. K. Kumar, and J. Bashnagel, *J. Chem. Phys.* **116**, 865 (2002).
- <sup>19</sup>R. Casalini, S. Capaccioli, M. Lucchesi, P. A. Rolla, and S. Corezzi, *Phys. Rev. E* **63**, 031207 (2001).
- <sup>20</sup>H. Vogel, *Phys. Z.* **222**, 645 (1921).
- <sup>21</sup>G. S. Fulcher, *J. Am. Ceram. Soc.* **8**, 339 (1923).
- <sup>22</sup>M. Paluch, J. Gapinski, A. Patkowski, and E. W. Fischer, *J. Chem. Phys.* **114**, 8048 (2001).
- <sup>23</sup>P. G. Tait, *Phys. Chem.* **2**, 1 (1888).
- <sup>24</sup>H. Schlosser and J. Ferrante, *J. Phys.: Condens. Matter* **1**, 2727 (1989).
- <sup>25</sup>D. W. VanKrevelen, *Properties of Polymers* (Elsevier, Amsterdam, 1997).
- <sup>26</sup>R. Simha, P. S. Wilson, and O. Olabisi, *Kolloid Z. Z. Polym.* **251**, 402 (1973).
- <sup>27</sup>R. Casalini and C. M. Roland, *J. Chem. Phys.* (to be published).
- <sup>28</sup>S. Corezzi, P. A. Rolla, M. Paluch, J. Ziolo, and D. Fioretto, *Phys. Rev. E* **60**, 4444 (1999).
- <sup>29</sup>M. Paluch, S. Hensel-Bielowka, and J. Ziolo, *Phys. Rev. E* **61**, 526 (2000).
- <sup>30</sup>M. Paluch, K. L. Ngai, and S. Henel-Bielowka, *J. Chem. Phys.* **114**, 10872 (2001).
- <sup>31</sup>D. J. Plazek and K. L. Ngai, *Macromolecules* **24**, 1222 (1991).
- <sup>32</sup>R. Böhmer, K. L. Ngai, C. A. Angell, and D. J. Plazek, *J. Chem. Phys.* **99**, 4201 (1993).
- <sup>33</sup>K. L. Ngai and C. M. Roland, *Macromolecules* **26**, 6824 (1993).
- <sup>34</sup>C. M. Roland and K. L. Ngai, *Macromolecules* **25**, 5765 (1992).
- <sup>35</sup>C. M. Roland and K. L. Ngai, *Macromolecules* **24**, 5315 (1991).
- <sup>36</sup>C. M. Roland and K. L. Ngai, *Macromolecules* **25**, 1844 (1992).
- <sup>37</sup>P. G. Santangelo, K. L. Ngai, and C. M. Roland, *Macromolecules* **29**, 3651 (1996).
- <sup>38</sup>C. M. Roland, *Macromolecules* **27**, 4242 (1994).
- <sup>39</sup>K. L. Ngai and C. M. Roland, *Macromolecules* **26**, 2688 (1993).
- <sup>40</sup>M. J. Schroeder and C. M. Roland, *Macromolecules* **35**, 2676 (2002).
- <sup>41</sup>A. Patkowski, M. Paluch, and H. Krieg, *J. Chem. Phys.* **117**, 2192 (2002).
- <sup>42</sup>M. Paluch, C. M. Roland, and S. Pawlus, *J. Chem. Phys.* **116**, 10932 (2002).
- <sup>43</sup>M. Paluch, S. Hensel-Bielowka, and J. Ziolo, *J. Chem. Phys.* **110**, 10978 (1999).
- <sup>44</sup>M. Paluch, R. Casalini, S. Hensel-Bielowka, and C. M. Roland, *J. Chem. Phys.* **116**, 9839 (2002).
- <sup>45</sup>F. Stickel, E. W. Fischer, and R. Richert, *J. Chem. Phys.* **102**, 6251 (1995).
- <sup>46</sup>R. Casalini, S. Capaccioli, M. Lucchesi, P. A. Rolla, M. Paluch, S. Corezzi, and D. Fioretto, *Phys. Rev. E* **64**, 041504 (2001).
- <sup>47</sup>O. Yamamuro, I. Tsukushi, A. Lindqvist, S. Takahara, M. Ishikawa, and T. Matsuo, *J. Phys. Chem. B* **102**, 1605 (1998).
- <sup>48</sup>R. Casalini, S. Capaccioli, M. Lucchesi, M. Paluch, S. Corezzi, and P. A. Rolla, *J. Non-Cryst. Solids* **307-310**, 270 (2002).